Jiang, L.H., Rassendren, F., Spelta, V., Surprenant, A., North, R.A., 2001. Amino acid residues involved in gating identified in the first membrane-spanning domain of the rat P2X$_2$ receptor. J. Biol. Chem. 276, 14902–14908.

Khakh, B.S., 2001. Molecular physiology of P2X receptors and ATP signalling at synapses. Nat. Rev. 2, 165–174.

Migita, K., Haines, W.R., Voigt, M.M., Egan, T.M., 2001. Polar residues of the second transmembrane domain influence cation permeability of the ATP-gated P2X$_2$ receptor. J. Biol. Chem. 276, 30934–30941.

Nakazawa, K., Ohno, Y., 1997. Effects of neuroamines and divalent cations on cloned and mutated ATP-gated channels. Eur. J. Pharmacol. 325, 101–108.

Nakazawa, K., Fujimori, K., Takanaka, A., Inoue, K., 1989. An ATP-activated conductance in pheochromocytoma cells and its suppression by extracellular calcium. J. Physiol. 428, 257–272.

Nakazawa, K., Liu, M., Inoue, K., Ohno, Y., 1997a. pH dependence of facilitation by neurotransmitters and divalent cations of P2X$_2$ purino-ceptor/channels. Eur. J. Pharmacol. 337, 309–314.

Nakazawa, K., Liu, M., Inoue, K., Ohno, Y., 1997b. Voltage-dependent gating of ATP-activated channels in PC12 cells. J. Neurophysiol. 78, 884–890.

Nakazawa, K., Ojima, H., Ohno, Y., 2002. A highly conserved tryptophane residue indispensable for cloned rat neuronal P2X receptor activation. Neurosci. Lett. 324, 141–144.

North, R.A., 2002. Molecular physiology of P2X receptors. Physiol. Rev. 82, 1013–1067.

North, R.A., Surprenant, A., 2000. Pharmacology of cloned P2X receptors. Annu. Rev. Pharmacol. Toxicol. 40, 563–580.

Ralevic, V., Burnstock, G., 1998. Receptors for purines and pyrimidines. Pharmacol. Rev. 50, 413–492.

Rassendren, F., Buell, G., Newbolt, A., North, R.A., Surprenant, A., 1997. Identification of amino acid residues contributing to the pore of a P2X receptor. EMBO J. 16, 3446–3454.

Roberts, J.A., Evans, R.J., 2004. ATP binding at human P2X$_1$ receptors. Contribution of aromatic and basic amino acids revealed using mutagenesis and partial agonists. J. Biol. Chem. 279, 9043–9055.

Rubio, M., Soto, F., 2001. Distinct localization of P2X receptors at excitatory postsynaptic specializations. J. Neurosci. 21, 641–653.

Weber, W.-M., 1999. Ion currents of Xenopus laevis oocytes: state of the art. Biochim. Biophys. Acta 1421, 213–233.

Zhang, Y., Hamill, O.P., 2000. Calcium, voltage- and osmotic stress sensitive currents in Xenopus oocytes and their relationship to single mechanically gated channels. J. Physiol. 523, 83–99.

Carbon monoxide protects cardiomyogenic cells against ischemic death through L-type Ca^{2+} channel inhibition

Koichi Uemura [a,*], Satomi Adachi-Akahane [b], Kaori Shintani-Ishida [a], Ken-ichi Yoshida [a]

[a] *Department of Forensic Medicine, Graduate School of Medicine, The University of Tokyo, 7-3-1 Hongo, Bunkyo-ku, Tokyo 113-0033, Japan*
[b] *Laboratory of Cell Signaling, Graduate School of Pharmaceutical Sciences, The University of Tokyo, 7-3-1 Hongo, Bunkyo-ku, Tokyo 113-0033, Japan*

Received 16 June 2005
Available online 5 July 2005

Abstract

Carbon monoxide (CO) is known to protect myocardial and vascular cells against injuries due to ischemia–reperfusion or inflammation. We showed that a Ca^{2+}-dependent protease calpain promotes necrotic cell death of cardiomyocyte-derived H9c2 cells due to hypoxia through α-fodrin proteolysis. Here, we show that ischemia induces necrotic cell death, which is inhibited by either CO, extracellular Ca^{2+} deprivation or L-type Ca^{2+} channel blockers. A whole cell patch-clamp experiment supports that CO inhibits L-type Ca^{2+} channel mediated influx of Ca^{2+} and the ischemic death of H9c2 cells.
© 2005 Published by Elsevier Inc.

Keywords: Carbon monoxide; Ischemia; Necrosis; L-type Ca^{2+} channel; Calpain

Ischemia–reperfusion induces injury and death of cardiomyocytes or cardiomyogenic cells through Ca^{2+} overloading, reactive oxygen species (ROS) generation, or mitochondrial depolarization [1]. We previously showed that Ca^{2+}-activated protease calpain causes injury in the isolated rat heart after ischemia–reperfusion [2–4] and cardiomyogenic H9c2 cells after hypoxia [5] or ischemia–reperfusion [6].

Carbon monoxide (CO) is the most prevalent lethal gas in the civilized countries, but several studies support the beneficial effects of CO in cardiomyocytes, vascular cells, and the heart under ischemia–reperfusion [7–9]. In addition, lipopolysaccharide (LPS) upregulates cytokines, adhesion molecules, and inducible NO synthase, thereby promoting cell death in endothelial cells. Exogenous or endogenous CO can suppress these responses to LPS [10] and prevent LPS-mediated lethality in the mice [11].

Heme-oxygenase-1 (HO-1) is induced by ROS or heme-metabolites [12]. HO-1 catalyzes the metabolism of heme-proteins to CO and bilirubin [13]. Additionally, it was reported that CO alleviates the vascular smooth muscle cell apoptosis by cytokines [14]. In the HO-1 knock-out mice, it was reported that hypoxia promotes right ventricular dilatation and infarction through lipid peroxidation and apoptosis [15], and that ischemia frequently induces ventricular fibrillation [16]. By contrast, cardiac-specific over-expression of HO-1 attenuates the inflammatory reactions in ischemia–reperfusion injury [17], whereas HO-1 over-expression by hemin-pretreatment protects the myocardium against infarction [18]. Recently, it was shown that a CO generator can protect cardiomyogenic H9c2 cells against hypoxia–reoxygenation injury, and the heart against ischemia–reperfusion injury [19].

In this study, we investigated whether and how CO protects cardiomyogenic H9c2 cells against ischemia with reference to Ca^{2+} overloading and ROS generation.

* Corresponding author. Fax: +81 3 5841 3366.
  E-mail address: kuemura@m.u-tokyo.ac.jp (K. Uemura).

Materials and methods

Materials. Fluo-3/AM was obtained from Dojindo Laboratories (Kumamoto, Japan), 5-hydroxydecanoic acid (5-HD) from Biomol Research Laboratory (Plymouth Meeting, PA), dichlorodihydrofluorescein diacetate (DCFH-DA) and DiBAC$_4$(3) were from Molecular Probe (Eugene, OR), hydroethidine from Polysciences (Warrington, PA). Hemin chloride was obtained from ICN Biochemicals (Aurora, Ohio), nifedipine, diltiazem, Hoechst 33342, and propidium iodide were from Wako Pure Chemical (Osaka, Japan). 1*H*-(1,2,4)Oxadiazolo(4,3-α)quinoxalin-1-one (ODQ), SB203580, and Bay K 8644 were purchased from Calbiochem (Darmstadt, Germany), and other reagents are commercially available. These reagents were dissolved in DMSO (0.1%). DMSO had no effect on the cell viability.

DMEM and FBS were purchased from Sigma Chemical (St. Louis, MO) and Thermo Trace (Melbourne, Australia), respectively. Other cell culture reagents were obtained from Invitrogen (Carlsbad, CA). The anti-α-fodrin antibody was obtained from Biohit PLC (Helsinki, Finland), and the secondary antibodies were from Promega (Madison, WI).

Cell culture. H9c2 cells derived from rat embryonic cardiomyocytes were grown to confluence (approx. 1×10^6 per dish in 60-mm culture dishes) in DMEM with 10% FBS at 37 °C.

Ischemia or CO exposure. The ischemic medium was prepared by bubbling Hepes-buffered salt solution (HBSS) containing (mM): NaCl, 125; KCl, 4.9; MgSO$_4$, 1.2; NaH$_2$PO$_4$, 1.2; CaCl$_2$, 1.8; NaHCO$_3$, 8.0; and Hepes, 20.0 (pH 7.4) [20] with N$_2$ gas for 30 min before each experiment. Ischemia was simulated by replacing the DMEM with the ischemic medium and maintaining the dishes under hypoxic gas (O$_2$/N$_2$/CO$_2$, 2.0/93/5%) in a multi-gas incubator (APM-30D, ASTEC, Fukuoka, Japan). For CO experiments, the ischemic medium was bubbled with the hypoxic-CO gas (CO/O$_2$/N$_2$/CO$_2$, 1.0/2.0/92/5%, Yamato Sanki, Tokyo) for 30 min. The DMEM was replaced with the ischemia-CO medium and the dishes were placed in a sealed chamber filled with the hypoxic-CO gas.

Cell viability assays. Dye-exclusion assay was performed using erythrosine B, as reported previously [21]. Plasma membrane integrity and nuclear morphology were observed under a fluorescence microscope (Eclipse TE-200E, Nikon, Tokyo, Japan) after treatment with propidium iodide (PI, 10 μg/ml) and Hoechst 33342 (100 μM), respectively.

Caspase-3 activity. Caspase-3 activity was measured with a kit (CaspACE Assay System Colorimetric, Promega, Madison, WI), according to the manufacturer's instruction.

Microplate fluorescence measurement of intracellular Ca^{2+} level (Ca$_i^{2+}$). Cells were plated at 1×10^4 per well and allowed to reach confluence for 2 days on black 96-well plates with transparent bottoms (Costar 3603, Corning, NY). The cells were loaded with 4.4 μM fluo-3/AM in a DMEM supplemented with 0.04% Pluronic F-127 for 1 h. After being washed with PBS, cells were exposed either to ischemia or CO + ischemia in the presence of 1.25 mM probenecid that prevents fluo-3 leakage. The fluorescence intensity for intracellular Ca^{2+} level (Ca$_i^{2+}$) was measured with excitation at 485 nm and emission at 535 nm by a fluorescence microplate reader (GENios, Tecan, Austria).

Electrophysiological recordings. Ca^{2+}-influx through the Ca^{2+} channel (I_{Ca}) was recorded at room temperature by whole cell patch-clamp configuration using an Axopatch 200B voltage-clamp amplifier (filtered at 2–5 kHz, sampled at 5–10 kHz). The computer was equipped with an A/D converter, Digidata 1200 (Axon Instruments), and pCLAMP ver.7.0 software (Axon Instruments) [22]. Borosilicated glass pipettes, filled with an internal solution, had a resistance of 1–3 MΩ. The observational resistance was less than one-third of the pipette resistance. The pipette solution contained (in mM): Cs-methanesulfonate, 120; TEACl, 20; Hepes, 10; Na$_2$-phosphocreatine, 5; Na-GTP, 0.2; Mg-ATP, 5 (pH 7.3). Cells were super-perfused with Tyrode solution composed of (in mM): NaCl, 137; KCl, 5.4; MgCl$_2$, 1; glucose, 10; Hepes, 10; CaCl$_2$, 2 (pH 7.4). The inward rectifier K$^+$ current was blocked with Ba^{2+} (0.2 mM). I_{Ca} was estimated from the difference between the currents in the absence and presence of Cd^{2+} (0.2 mM).

Reactive oxygen species measurement. Dichlorofluorescein (DCF) is a non-specific reactive oxygen species (ROS) indicator. Cells on 60-mm dishes were incubated with DCFH-DA (10 μM) for 30 min. After ischemia or CO exposure, the cells were harvested and dissolved in 50% dimethylsulfoxide (DMSO). The DCF fluorescence was measured with a fluorospectrometer (RF-1500, Schimadzu, Kyoto, Japan) with excitation at 480 nm and emission at 530 nm [23].

Hydroethidine is relatively specific for O$_2^-$. The cells grown on the 96-well plates were pre-incubated in 20 μM hydroethidine for 1 h, washed with PBS, and then underwent ischemia or CO exposure. The fluorescence was determined with excitation at 535 nm and emission at 595 nm.

H$_2$O$_2$ was measured with Amplex Red and HRP using an Amplex Red Hydrogen Peroxide Assay kit (Molecular Probe, Eugene, OR), according to the manufacturer's instructions.

Plasma membrane potential. The cells grown on 96-well plates were pre-incubated in 5 μM DiBAC$_4$(3) for 30 min before ischemia or CO exposure. The fluorescence of the plasma membrane potential was monitored for 30 min with excitation at 485 nm and emission at 535 nm.

Electrophoresis and Western blotting. After ischemia or exposure to CO, the cells on 60-mm dishes were harvested. The extract was prepared from these cells including floating cells [21]. The extract (12.5 μg protein per lane) was subjected to SDS–polyacrylamide gel electrophoresis according to Laemmli [24], using 6.5% gels for anti-α-fodrin. Protein was determined by the Coomassie method (Pierce, Rockford, IL). Western blotting was performed according to Towbin et al. [25], using a Western Lightning Chemiluminescence Reagent Plus kit (Perkin Elmer Life Sciences, Boston, MA). The band densities were measured with an image analyzer (Densitograph AE-6905C; Atto, Tokyo, Japan) and expressed as percentage of the mean value of the control.

Statistics. Data are expressed as means ± SD. Statistical analyses were performed by analysis of variance (ANOVA), followed by Fischer's post hoc analysis. Values of $p < 0.05$ were considered statistically significant.

Results

CO protected the H9c2 cells against ischemia, as demonstrated by the dye-exclusion assay (Fig. 1A). The cell death was characterized as necrotic by double staining with Hoechst and PI. The red PI staining of ischemic cells showed plasma membrane hyper-permeability, due either to necrosis or advanced apoptosis (Fig. 1B). CO suppressed PI staining of ischemic cells (Fig. 1B). By contrast, apoptotic changes such as chromatin condensation, shrinkage, and nuclear fragmentation, as detected by Hoechst 33342 staining, were not found in ischemia, but in staurosporine-treated cells (Fig. 1B). Caspase-3, the key executor protease of apoptosis, was not activated by ischemia, but by staurosporine (Fig. 1C). Thus, ischemic death of H9c2 cells is predominantly necrotic and CO suppressed the death.

Ischemic cell death was inhibited by CO at least partly through inhibition of a Ca^{2+}-dependent protease calpain. We showed previously that α-fodrin, a predominant substrate for calpain, was degraded to
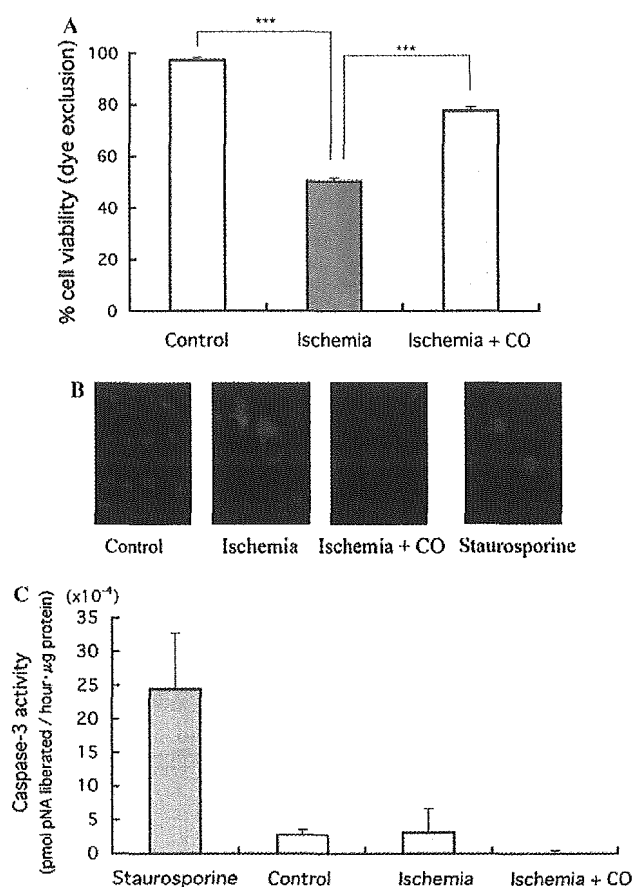
Fig. 1. Effects of CO on ischemic death. (A) The viability of cells cultured under normoxia, ischemia (2% O_2), or CO-ischemia (1% CO, 2% O_2) for 16 h was measured by dye exclusion. Data are expressed as means ± SD, $n = 4$. ***$p < 0.001$. (B) Double staining with propidium iodide (PI) and Hoechst 33342. Ischemic cells showed red staining with PI, due to hyper-permeability of the cell membrane (necrosis), but not nuclear changes in Hoechst 33342 staining (blue) (apoptosis). Stauro-sporine-treated cells showed nuclear changes due to apoptosis. (C) Caspase-3 activity (means ± SD, $n = 4$–5) of cells underwent ischemia or CO-ischemia for 14 h, and staurosporine-treated cells were used as a positive control.
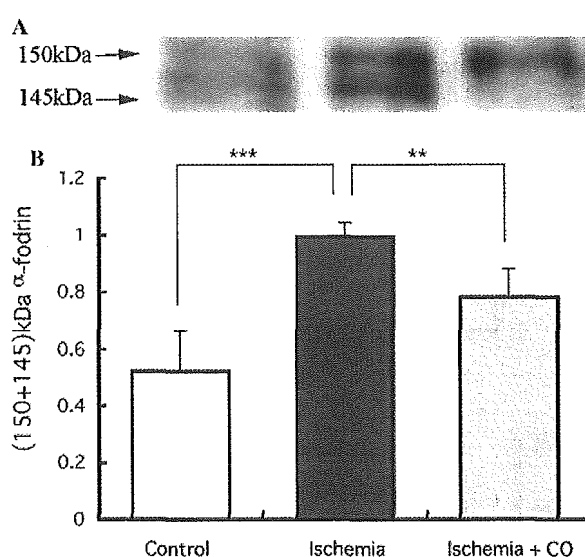

Fig. 2. Effect of CO on α-fodrin degradation in ischemia. The cells were cultured under normoxia, ischemia, or CO-ischemia for 24 h. (A) A representative Western blot of α-fodrin degradation. (B) Semi-quantification of the 150/145 kDa fragments of α-fodrin. Data are expressed as means ± SD, $n = 4$. **$p < 0.01$. ***$p < 0.001$.

generate 150/145 kDa fragments in the heart after ische-mia–reperfusion and in H9c2 cells after hypoxia [3,5]. The 150/145 kDa fragments of α-fodrin are hallmark of necrosis [26]. We confirmed the α-fodrin degradation by ischemia and its inhibition by CO (Fig. 2).

The cell death was suppressed by deprivation of Ca^{2+} from the ischemia medium, demonstrated by the dye-ex-clusion assay (Fig. 3A). Likewise, L-type Ca^2 channel blockers, nifedipine (10 μM) and diltiazem (10 μM), alleviated ischemic cell death, as did CO (Fig. 3B).

These observations led us to examine the intracellular Ca^{2+} level (Ca_i^{2+}) by fluo-3/AM (Fig. 4A). The basal Ca_i^{2+} was lower in the presence of CO than in its ab-sence. As reported previously [1], ischemia increased the basal Ca_i^{2+} level (Fig. 4A). Notably, CO alleviated

the Ca^{2+} overloading of ischemic cells in a concentra-tion-dependent manner (Fig. 4A). It was reported that saturated CO solution contains approximately 1 mM CO [27].

The two L-type Ca^{2+} channel blockers reduced Ca^{2+} overloading in ischemia (Fig. 4B). CO suppressed the Ca^{2+} overloading more efficiently than these blockers. Additionally, CO inhibited the Ca^{2+} overloading evoked by Bay K 8644, a L-type Ca^{2+} channel agonist (Fig. 4C). These data suggest that CO attenuates Ca^{2+} overloading in ischemic cells by inhibition of Ca^{2+}-influx through the L-type Ca^{2+} channel. Recently, Lim et al. [28] reported that CO activates human intestinal smooth muscle L-type Ca^{2+} channels through a nitric oxide (NO)-de-pendent mechanism. However, we found neither expres-sion of endothelial NO synthase (eNOS) or inducible NO synthase (iNOS) in H9c2 cells, nor inhibition by a NOS inhibitor, N^{ω}-nitro-L-arginine (L-NAME) on Ca_i^{2+} level (data not shown). Additionally, an inhibitor for guanylate cyclase (1H-(1,2,4)oxadiazolo(4,3-a)qui-noxalin-1-one: ODQ; 1 μM) did not affect the viability or Ca_i^{2+} level in ischemic cells (data not shown).

Whole cell patch-clamp experiments confirmed that CO reduced the L-type Ca^{2+} channel currents (I_{Ca}) in normoxic cells (Figs. 5A and B). Notably, the Ca^{2+} cur-rents altered within seconds after CO application and were recovered by 10 min after wash out (Fig. 5B). CO also reduced I_{Ca} density to 44.5 ± 8.3% ($n = 6$, $p < 0.01$) of the control (Fig. 5C). Although we could not measure I_{Ca} under ischemia due to technical difficul-ties, these experiments strongly support the contribution
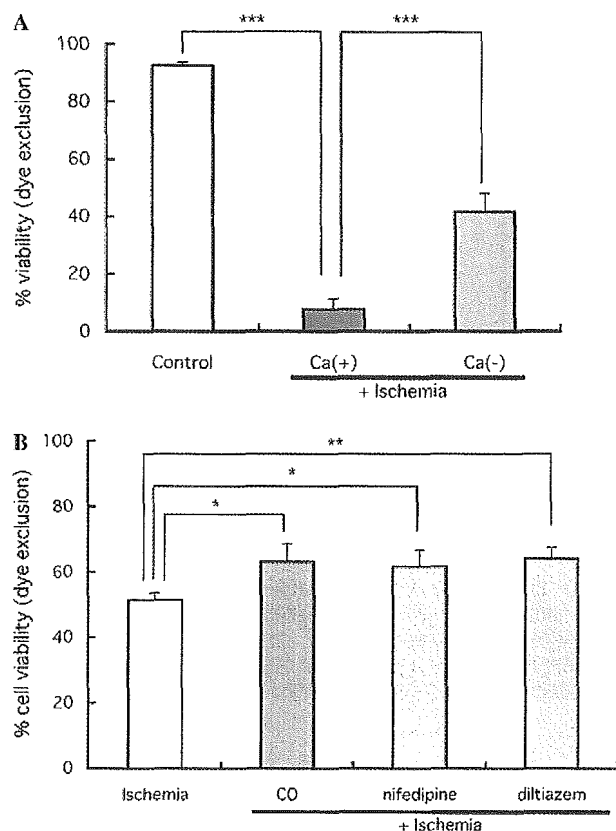
A

B

Fig. 3. Effect of Ca^{2+} on cell viability. (A) The ratio of viable cells with dye exclusion after culture under normoxia, ischemia, and ischemia with Ca^{2+} deprivation for 24 h. Data are expressed as means ± SD, $n = 4$. ***$p < 0.001$. (B) The ratio of viable cells with dye exclusion of cells cultured under ischemia alone or in the presence of CO, nifedipine (10 μM), or diltiazem (10 μM) for 24 h. Data are expressed as means ± SD, $n = 4$. *$p < 0.05$. **$p < 0.01$.

of inhibition of L-type Ca^{2+} channel by CO to the alleviation of Ca^{2+} overloading and cell death in ischemia.

Reactive oxygen species (ROS) are generated by mitochondrial respiratory inhibition under ischemia [29], whereas CO inhibits mitochondrial complex IV [30]. Additionally, ROS modulates L-type Ca^{2+} channel activity [31]. Therefore, we measured ROS in ischemia. We confirmed that ischemia enhanced ROS production in ischemia as detected by a non-specific ROS indicator DCF. However, CO did not modulate the ROS production in ischemia (Fig. 6A). Similar results were obtained for hydroethidine fluorescence, the indicator relatively specific for O$_2$ (Fig. 6B) and for Amplex Red fluorescence, the indicator specific for H$_2$O$_2$ production (Fig. 6C). These results suggest that the effect of CO is not related to ROS.

Recently, a mitochondrial ATP-dependent K$^+$ channel inhibitor (5-hydroxydecanoate: 5-HD) was shown to blunt the protective effect of CO on H9c2 cells under hypoxia–reoxygenation [19]. However, 5-HD did not inhibit the CO-mediated protection against ischemic cell death (Fig. 7).
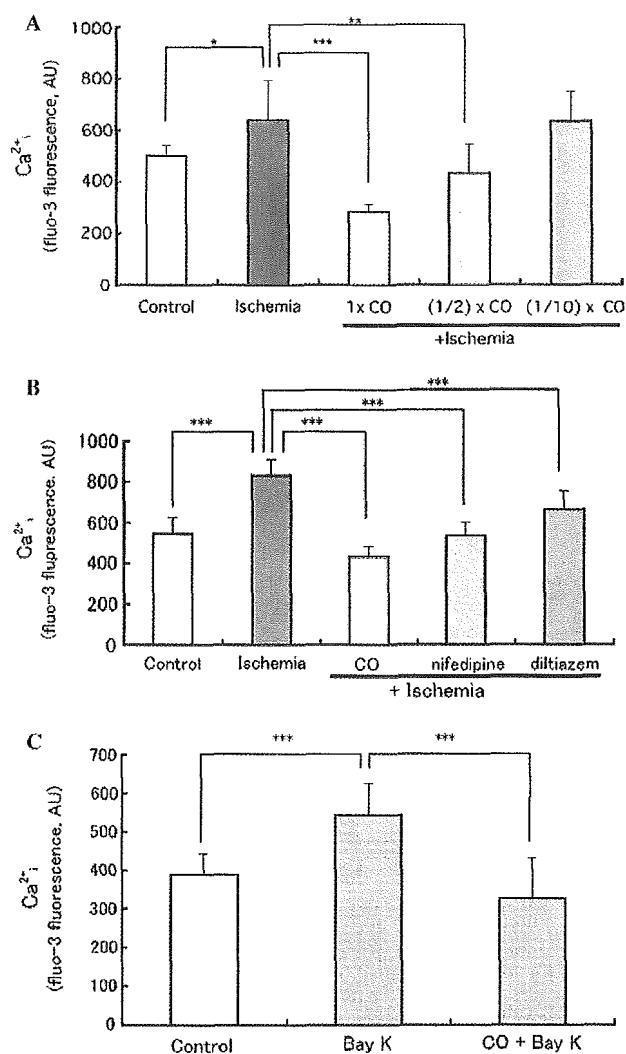
A

B

C

Fig. 4. Effect of CO, L-type Ca^{2+} blockers, and Bay K 8644 on intracellular Ca^{2+} levels (Ca$_i$$^{2+}$). (A) Ischemia for 1 h increased intracellular Ca^{2+} (Ca$_i$$^{2+}$) as detected by fluo-3 fluorescence. CO reduced Ca$_i$$^{2+}$ overloading due to ischemia in a concentration-dependent manner. Data are expressed as means ± SD, $n = 8$. (B) L-type Ca^{2+} channel blockers, nifedipine (10 μM), and diltiazem (10 μM) also reduced the Ca^{2+} overloading. Data are expressed as means ± SD, $n = 8$. (C) A L-type Ca^{2+} channel agonist, Bay K 8644 (1 μM), elevated Ca$_i$$^{2+}$ after 1 h, but CO suppressed the increase. Data are expressed as means ± SD, $n = 4$–8. *$p < 0.05$. **$p < 0.01$. ***$p < 0.001$.

CO and NO were shown to relax vascular smooth muscle cells through activation of large conductance Ca^{2+}-activated K$^+$ channels or guanylate cyclase [32]. The activation of Ca^{2+}-activated K$^+$ channels causes plasma membrane hyperpolarization, as detected by Di-BAC$_4$(3). However, we did not detect such a change in ischemic H9c2 cells (data not shown).

It was shown that CO protects the myocardium, endothelium, and macrophage against cell death induced by ischemia–reperfusion, TNF-α, IL-10 or LPS through p38MAP kinase modulation [7,10,11,33,34].
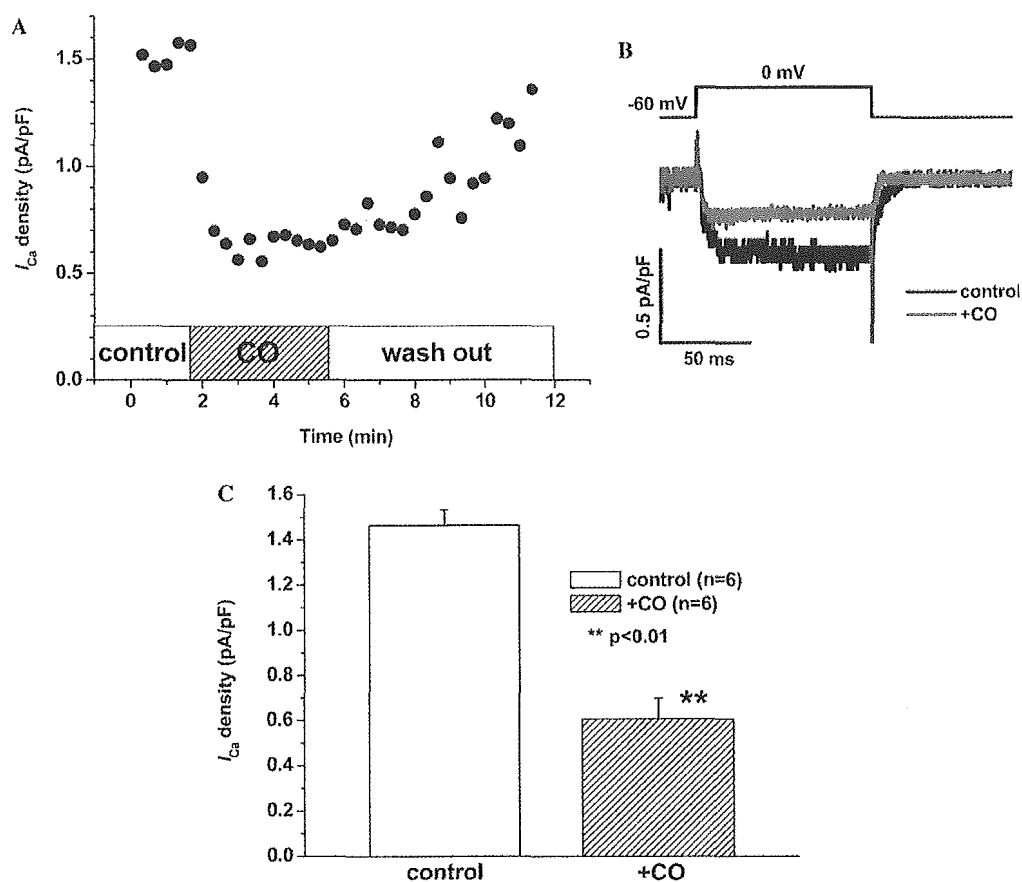
Fig. 5. CO attenuated Ca^{2+} channel currents (I_{Ca}). (A) Effect of CO on Ca^{2+} channel currents (I_{Ca}) as monitored by a whole cell patch clamp. The superfusion medium was switched from normal Tyrode to a CO-saturated Tyrode solution during the period indicated by the horizontal bar, and washed with normal Tyrode. (B) Typical I_{Ca} traces recorded before (black line) and during (gray line) the application of the CO-saturated solution. (C) Summary of the effect of CO on L-type Ca^{2+} channel current. CO reduced I_{Ca} density to $44.5 + 8.3\%$ ($n = 6$, $p < 0.01$) of the control level. ** $p < 0.01$.

However, a p38MAP kinase inhibitor, SB203580 (4 μM), did not inhibit the protective effect of CO in ischemic H9c2 cells (data not shown).

Discussion

This study provides the first line of evidence that CO suppresses Ca^{2+}-influx through L-type Ca^{2+} channel (I_{Ca}) and thereby attenuates necrotic death (Figs. 1–3) of ischemic cardiomyogenic H9c2 cells. The effect of CO on the Ca^{2+} channel was demonstrated by the intracellular Ca^{2+} (Ca_i^{2+}) monitoring by fluo-3 (Fig. 4), and by a whole cell patch-clamp configuration (Fig. 5).

CO relaxes vascular smooth muscle cells either via a cGMP-dependent pathway [12,35,36], a Ca^{2+}-activated K^+ channel [27,37], or NO. We found no evidence for the involvement of cGMP-dependent kinase, or Ca^{2+}-activated K^+ channel. Recently, it was reported that CO activates L-type Ca^{2+} channel through NO activation [28]. However, as they argued that there are tissue

and species differences, we found no evidence for involvement of NO in the CO-mediated L-type Ca^{2+} channel activation. Thus, the effect of CO on ischemic H9c2 cells was not mediated through either of NO, cGMP, or Ca^{2+}-activated K^+ channel.

Recently, it was reported that the mitochondrial ATP-dependent K^+ channel is involved in the protection afforded by CO in H9c2 cells or the isolated heart against ischemia–reperfusion [19]. However, the same mitochondrial ATP-dependent K^+ channel inhibitor had no effect on the protection by CO in ischemic H9c2 cells (Fig. 7). Different mechanisms would underlie protection afforded by CO against ischemia and ischemia–reperfusion, as shown by the reports that Na^+/H^+-exchanger promotes Ca^{2+}-influx and mitochondrial dysfunction in reperfusion but not in ischemia [38,39]. On the other hand, CO attenuates progression of apoptosis by TNF-α or ischemia–reperfusion [10,33], and inflammatory responses to IL-10 and LPS [11,34], through p38 MAP kinase inhibition. However, p38 MAP kinase inhibition did not suppress the effect of CO on ischemic H9c2 cells.
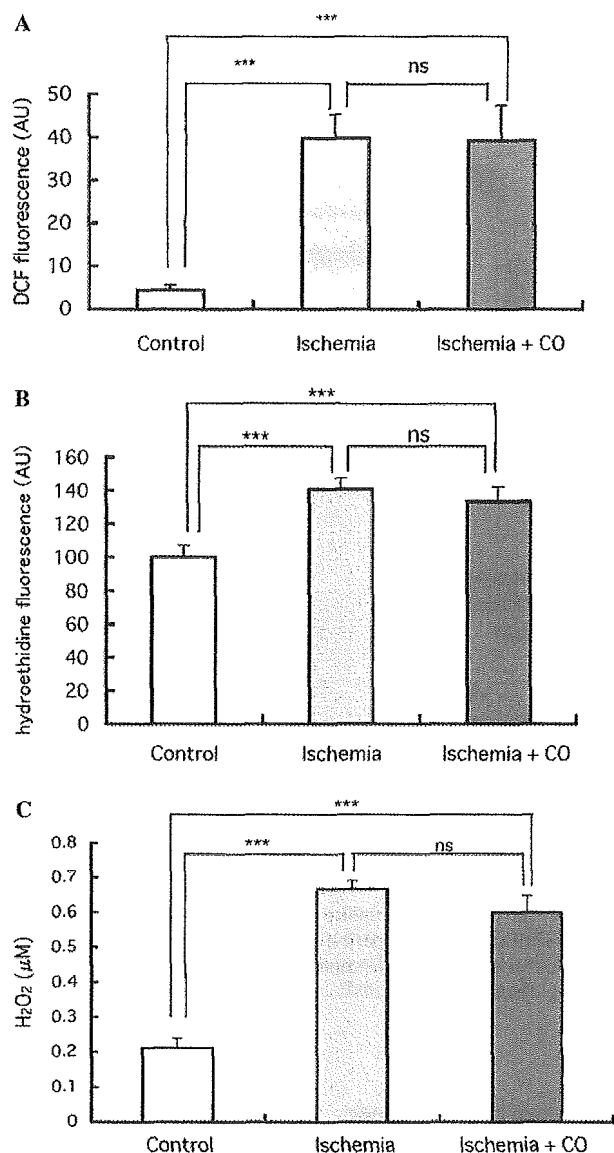
A

B

C

Fig. 6. Effect of CO on reactive oxygen species (ROS) production in ischemia. ROS production was enhanced by ischemia (3 h), but unaffected by CO, as detected by DCF (A, non-specific), hydroethidine (B, O_2^--specific), or Amplex Red Hydrogen Peroxide (C, H_2O_2-specific). ***$p < 0.001$. ns, not significant.
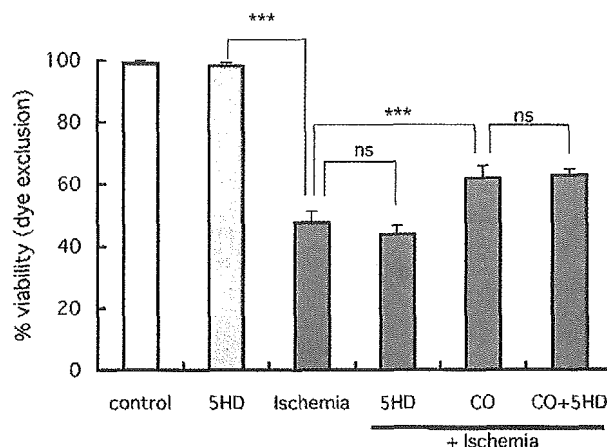

Fig. 7. Effect of a mitochondrial ATP-dependent K^+ (K_{ATP}) channel blocker on cell death after ischemia. 5-Hydroxydecanoic acid (5-HD, 50 μM), a K_{ATP} channel blocker, did not blunt the protective effect of CO against ischemic death (20 h), as measured by dye exclusion. Data are expressed as means ± SD, $n = 4,5$. ***$p < 0.001$. ns, not significant.

The most important finding of this study is that CO directly inhibits L-type Ca^{2+} channel in H9c2 cells. The effect of CO on L-type Ca^{2+} channel was rapid upon application and reversible after washing (Fig. 5A). The latter suggests that this effect is not mediated through a heme-protein with well-known high affinity for CO. However, we cannot exclude the possibility that CO modulates topologically located amino acid residues on L-type Ca^{2+} channel, as was shown for the Ca^{2+}-activated K^+ channels of smooth muscle cells [27].

Consistent with the suppression of the Ca^{2+} overloading by CO in ischemic cells, CO inhibited the

proteolysis of α-fodrin (Fig. 2), a well-known substrate for Ca^{2+}-dependent protease calpain [3]. In addition, the ischemic death of H9c2 cells was necrotic (Fig. 1), which was shown to be promoted by Ca^{2+} overloading and calpain activation [5]. Consistent with the results of this study, we previously showed in the perfused rat heart after ischemia–reperfusion that L-type Ca^{2+} channel blocker, verapamil, inhibits calpain activation and creatine kinase release [40], while a calpain inhibitor inhibits α-fodrin degradation, and myocardial contractile dysfunction [3]. Verapamil was also shown to inhibit myocardial apoptosis in ischemia–reperfused heart [41]. Moreover, L-type Ca^{2+} channel blockade attenuates infarct progression, through a calpain inhibition, in the rat heart after permanent coronary occlusion [42].

It was shown that H_2O_2 activates L-type Ca^{2+} channel in cardiomyocytes [31]. However, the contribution of H_2O_2 to the effect of CO on Ca^{2+}-influx is unlikely, since H_2O_2 generation was enhanced in ischemic H9c2 cells (Fig. 6), but CO did not inhibit the generation of H_2O_2 or other ROSs (Fig. 6).

We found that exogenous CO protected H9c2 cells against ischemic insult. Consistent with the result, we recently showed that CO inhalation protects the heart in in vivo ischemia–reperfusion of the rat [7]. It was also shown that a water soluble CO-releasing molecule (CORM) tricarbonylchloro(glycinato) ruthenium (II) (CORM-3) attenuates H9c2 cell death after hypoxia–reoxygenation or against a ROS generator paraquart [19] and that CORM-3 alleviates myocardial dysfunction and infarction after ischemia–reperfusion in mice [8]. On the other hand, we have evidence for the ability of HO-1-derived endogenous CO in the L-type Ca^{2+} channel activation, but further study is required to confirm the finding and elucidate the mechanism.

In conclusion, we showed that exogenous CO can protect myogenic cells against ischemic cell death (necrosis) through inhibition of L-type Ca^{2+} channel current and calpain activation.

References

[1] W.G. Waypa, J.D. Marks, M.M. Mack, C. Boriboun, P.T. Mungai, P.T. Schumacker, Mitochondrial reactive oxygen species trigger calcium increases during hypoxia in pulmonary arterial myocytes, Circ. Res. 91 (2002) 719–726.

[2] K. Yoshida, K. Harada, Proteolysis of erythrocyte-type and brain-type ankyrins in rat heart after postischemic reperfusion, J. Biochem. 122 (1997) 279–285.

[3] K. Yoshida, M. Inui, K. Harada, T. Saido, Y. Sorimachi, T. Ishihara, S. Kawashima, K. Sobue, Reperfusion of rat heart after brief ischemia induces proteolysis of calspectin (noneryth-roid spectrin or fodrin) by calpain, Circ. Res. 77 (1995) 603–610.

[4] K. Yoshida, Y. Yamasaki, S. Kawashima, Calpain activity alters in rat myocardial subfractions after ischemia or reperfusion, Biomed. Biochim. Acta 1182 (1993) 215–220.

[5] T. Aki, K. Yoshida, T. Fujimiya, Phosphoinositide 3-kinase accelerates calpain-dependent Proteolysis of fodrin during hypoxic cell death, J. Biochem. 132 (2002) 921–926.

[6] Y. Mizukami, S. Kobayashi, F. Uberall, K. Hellbert, N. Kobayashi, K. Yoshida, Nuclear mitogen-activated protein kinase activation by protein kinase C zeta during reoxygenation after ischemic hypoxia, J. Biol. Chem. 275 (2000) 19921–19927.

[7] H. Fujimoto, M. Ohno, S. Ayabe, H. Kobayashi, N. Ishizaka, H. Kimura, K. Yoshida, R. Nagai, Carbon monoxide protects against cardiac ischemia–reperfusion injury in vivo via MAPK and Akt–eNOS pathways, Arterioscler. Thromb. Vasc. Biol. 24 (2004) 1848–1853.

[8] Y. Guo, A.B. Stein, W.J. Wu, W. Tan, X. Zhu, Q.H. Li, B. Dawn, R. Motterlini, R. Bolli, Administration of CO-releasing molecule at the time of reperfusion reduces infarct size in vivo, Am. J. Physiol. Heart Circ. Physiol. 286 (2004) H1649–H1653.

[9] S.W. Ryter, L.E. Otterbein, Carbon monoxide in biology and medicine, Bioessays 26 (2004) 270–280.

[10] S. Brouard, P.O. Berbera, E. Tobiasch, M.P. Seldon, F.H. Bach, M.P. Soares, Heme-oxygenase-1-derived carbon monoxide requires the activation of transcription factor NF-κ B to protect endothelial cells from tumor necrosis factor-α-mediated apoptosis, J. Biol. Chem. 277 (2002) 17950–17961.

[11] T.S. Lee, Y.C. Lee, Heme oxygenase-1 mediates the anti-inflammatory effect of interleukin-10 in mice, Nature Med. 8 (2002) 240–246.

[12] T. Yoshida, P. Biro, T. Cohen, R.M. Muller, S. Shibahara, Human heme oxygenase cDNA and induction of its mRNA by hemin, Eur. J. Biochem. 171 (1988) 457–461.

[13] M.D. Mainees, Heme oxygenase: function, multiplicity, regulatory mechanisms, and clinical applications, FASEB J. 2 (1988) 2557–2568.

[14] X.L. Liu, G.B. Chapman, K.J. Peyton, A.I. Schafer, W. Durante, Carbon monoxide inhibits apoptosis in vascular smooth muscle cells, Cardiovasc. Res. 55 (2002) 396–405.

[15] S.F. Yet, M.A. Perrella, M.D. Layne, C.M. Hsieh, K. Maemura, L. Kobzik, P. Wiesel, H. Christou, S. Kourembanas, M.E. Lee, Hypoxia induces severe right ventricular dilatation and infarction in heme oxygenase-1 null mice, J. Clin. Invest. 103 (1999) 23–29.

[16] I. Bak, L. Szendrei, T. Turoczi, G. Papp, F. Joo, D.K. Das, J. de Leiris, P. Der, B. Juhasz, E. Varga, I. Bacskay, J. Balla, P. Kovacs, A. Tosaki, Heme oxygenase-1 related carbon monoxide production and ventricular fibrillation in isolated ischemic/reperfused mouse myocardium, FASEB J. 17 (2003) 2133–2135.

[17] S.F. Yet, R. Tian, M.D. Layne, Z. Wang, K. Maemura, M. Solovyeva, B. Ith, L.G. Melo, L. Zhang, J.S. Ingwall, V.J. Dzau, M.E. Lee, M.A. Perrella, Cardiac-specific expression of heme oxygenase-1 protects against ischemia and reperfusion injury in transgenic mice, Circ. Res. 89 (2001) 168–173.

[18] M. Hangaishi, N. Ishizaka, T. Aizawa, Y. Kurihara, J. Taguchi, R. Nagai, S. Kimura, M. Ohno, Induction of heme oxygenase-1 can act protectively against cardiac ischemia/reperfusion in vivo, Biochem. Biophys. Res. Commun. 279 (2000) 582–588.

[19] J.E. Clark, P. Naughton, S. Shurey, C.J. Green, T.R. Johnson, B.E. Mann, R. Foresti, R. Motterlini, Cardioprotective actions by a water-soluble carbon monoxide-releasing molecule, Circ. Res. 93 (2003) e2–e8.

[20] E. Karwatowska-Prokopczuk, J.A. Nordberg, H.L. Li, R.L. Engler, R.A. Gottlieb, Effect of vascular proton ATPase on pH$_i$, Ca^{2+}, and apoptosis in neonatal cardiomyocytes during metabolic inhibition/recovery, Circ. Res. 82 (1998) 1139–1144.

[21] K. Uemura, T. Aki, K. Yamaguchi, K. Yoshida, Protein kinase C-ε protects PC12 cells against methamphetamine-induced death: possible involvement of suppression of glutamate receptor, Life Sci. 72 (2003) 1595–1607.

[22] S. Yamaguchi, Y. Okamura, T. Nagao, S. Adachi-Akahane, Serine residue in the IIIS5-S6 linker of the L-type Ca^{2+} channel α_{1c} subunit is the critical determinant of the action of dihydropyridine Ca^{2+} channel agonists, J. Biol. Chem. 275 (2000) 41504–41511.

[23] B. Witenberg, H.H. Kalir, Z. Raviv, Y. Kletter, V. Kravtsov, I. Fabian, Inhibition by ascorbic acid of apoptosis induced by oxidative stress in HL-60 myeloid leukemia cells, Biochem. Pharm. 57 (1999) 823–832.

[24] U.K. Laemmli, Cleavage of structural proteins during the assembly of the head of bacteriophage T4, Nature 227 (1979) 680–685.

[25] H. Towbin, T. Staehelin, J. Gordon, Electrophoretic transfer of proteins from polyacrylamide gels to nitrocellulose sheets: procedure and some applications, Proc. Natl. Acad. Sci. USA 76 (1979) 4350–4354.

[26] K. Shiraishi, K. Naito, K. Yoshida, Inhibition of calpain but not caspase protects the testis against injury after experimental testicular torsion of rat, Biol. Reprod. 63 (2000) 1538–1548.

[27] R. Wang, L. Wu, The chemical modification of K$_{Ca}$ channels by carbon monoxide in vascular smooth muscle cells, J. Biol. Chem. 272 (1997) 8222–8226.

[28] I. Lim, S.J. Gibbons, G.L. Lyford, S.M. Miller, P.R. Strege, M.G. Sarr, S. Chatterjee, J.H. Szurszewski, V.H. Shar, G. Farrugia, Carbon monoxide activates human intestinal smooth muscle L-type Ca^{2+} channels through a nitric oxide-dependent mechanism, Am. J. Physiol. Gastrointest. Liver Physiol. 288 (2005) G7–G14.

[29] J. Duranteau, N.S. Chandel, A. Kulisz, Z. Shao, P.T. Schumacker, Intracellular signaling by reactive oxygen species during hypoxia in cardiomyocytes, J. Biol. Chem. 273 (1998) 11619–11624.

[30] D. Pankow, W. Ponsold, Effect of carbon monoxide exposure on heart cytochrome c oxidase activity of rats, Biomed. Biochim. Acta 43 (1984) 1185–1189.

[31] L.C. Hool, P.G. Arthur, Decreasing cellular hydrogen peroxide with catalase mimics the effects of hypoxia on the sensitivity of the L-type Ca^{2+} channel to β-adrenergic receptor stimulation in cardiac myocytes, Circ. Res. 91 (2002) 601–609.

[32] L. Wu, K. Cao, Y. Lu, R. Wang, Different mechanisms underlying the stimulation of K_{Ca} channels by nitric oxide and carbon monoxide, J. Clin. Invest. 110 (2002) 691–700.

[33] X. Zhang, P. Shan, L.E. Otterbein, J. Alam, R.A. Flavell, R.J. Davis, A.M.K. Choi, P.J. Lee, Carbon monoxide inhibition of apoptosis during ischemia–reperfusion lung injury is dependent on the p38 mitogen-activated protein kinase pathway and involves caspase 3, J. Biol. Chem. 278 (2003) 1248–1258.

[34] L.E. Otterbein, F.H. Bac, J. Alam, M. Soares, H.T. Lu, M. Wysk, R.J. Davis, R.A. Flavell, A.M.K. Choi, Carbon monoxide has anti-inflammatory effects involving the mitogen-activated protein kinase pathway, Nature Med. 6 (2000) 422–428.

[35] X.L. Liu, G.B. Chapman, K.J. Peyton, A.I. Schafer, W. Durante, Antiapoptotic action of carbon monoxide on cultured vascular smooth muscle cells, Exp. Biol. Med. 228 (2003) 572–575.

[36] S. Kwon, S. Chumg, D. Ahn, D. Yeon, T. Nam, Mechanisms of carbon monoxide-induced relaxation in the guinea pig ileal smooth muscle, J. Vet. Med. Sci. 63 (2001) 389–393.

[37] J.H. Jaggar, C.W. Leffler, S.Y. Cheranov, D. Tcheranova, E. Shuyu, X. Cheng, Carbon monoxide dilates cerebral arterioles by enhancing the coupling of Ca^{2+} sparks to Ca^{2+}-activated K^+ channels, Circ. Res. 91 (2002) 610–617.

[38] H.M. Piper, C. Balser, Y.V. Ladilov, M. Schafer, B. Siegmund, M. Ruiz-Meana, D. Garcia-Dorado, The role of Na^+/H^+ exchange in ischemia–reperfusion, Basic Res. Cardiol. 91 (1996) 191–202.

[39] S. Yamamoto, K. Matsui, N. Ohashi, Protective effect of Na^+/H^+ exchange inhibitor, SM-20550, on impaired mitochondrial respiratory function and mitochondrial Ca^{2+} overload in ischemic/reperfused rat hearts, J. Cardiovasc. Pharmacol. 39 (2002) 569–575.

[40] K. Yoshida, Y. Sorimachi, M. Fujiwara, K. Hironaka, Calpain is implicated in rat myocardial injury after ischemia or reperfusion, Jpn. Circ. J. 59 (1995) 40–48.

[41] F. Gao, B. Gong, T.A. Christopher, B.L. Lopez, A. Karasawa, X.L. Ma, Anti-apoptotic effect of benidipine, a long-lasting vasodilating calcium antagonist, in ischaemic/reperfused myocardial cells, Br. J. Pharmacol. 132 (2001) 869–878.

[42] S. Sandmann, J. Spormann, F. Prenzel, L. Shaw, T. Unger, Calcium channel blockade limits transcriptional, translational and functional up-regulation of the cardiac calpain system after myocardial infarction, Eur. J. Pharmacol. 453 (2002) 99–109.

Genetic Polymorphisms and Haplotypes of the Human Cardiac Sodium Channel α Subunit Gene (*SCN5A*) in Japanese and their Association with Arrhythmia

K. Maekawa[1,2,*], Y. Saito[1,2], S. Ozawa[1,3], S. Adachi-Akahane[4], M. Kawamoto[5], K. Komamura[6,7], W. Shimizu[6], K. Ueno[8], S. Kamakura[6], N. Kamatani[5], M. Kitakaze[6] and J. Sawada[1,2]

[1]*Project Team for Pharmacogenetics* [2]*Division of Biochemistry and Immunochemistry* [3]*Division of Pharmacology, National Institute of Health Sciences, Setagaya-ku, Tokyo, Japan*
[4]*Laboratory of Cell Signaling, Graduate school of Pharmaceutical Sciences, The University of Tokyo, Bunkyo-ku, Tokyo, Japan*
[5]*Division of Genomic Medicine, Department of Advanced Biomedical Engineering and Science, Tokyo Women's Medical University, Tokyo, Japanv*
[6]*Department of Cardiology* [7]*Department of Cardiovascular Dynamics Research Institute* [8]*Department of Pharmacy, National Cardiovascular Center, Suita, Japan*

Summary

Genetic variations in cardiac ion channels have been implicated not only as the causes of inherited arrhythmic syndromes, but also as genetic risk factors for some acquired arrhythmias. To elucidate the potential roles of genetic polymorphisms of the α subunit of the voltage-gated sodium channel type V (*SCN5A*) in cardiac rhythm disturbance, the entire *SCN5A* coding exons and their flanking introns were sequenced in 166 Japanese arrhythmic patients and 232 healthy controls. We detected 69 genetic variations, including 54 novel ones. Out of the 12 novel nonsynonymous single nucleotide polymorphisms (SNPs), p.Leu1988Arg was found at a frequency of 0.015. The other 11 SNPs were rare (0.001), with 6 found in arrhythmic patients and 5 in healthy controls. The frequency of a novel intronic SNP, c.703+130G>A, was significantly higher in the patients than in the controls, suggesting this SNP is associated with an unknown risk factor for arrhythmia. Following linkage disequilibrium analysis, the haplotype structure of *SCN5A* was inferred using high-frequency SNPs. The frequency of the haplotype harbouring both p.Leu1988Arg and the common SNP p.His558Arg (haplotype GG) was significantly lower in the patients than in the controls. This finding suggests that this haplotype (GG) might have been positively selected in the controls because of its protective effect against arrhythmias. This study provides fundamental information necessary to elucidate the effect of genetic variations in *SCN5A* on channel function and cardiac rhythm in Japanese, and probably in the Asian population.

Keywords: Cardiac arrhythmia, *SCN5A*, SNP, haplotype, Japanese

Introduction

Voltage–gated cardiac sodium (Na$^+$) channels produce cationic currents that are responsible for the rapid up-stroke of the cardiac action potential, and play a central role in the excitability of myocardial cells (Balser, 1999).

Correspondence: Keiko Maekawa, Ph.D., Division of Biochemistry and Immunochemistry, National Institute of Health Sciences, 1-18-1 Kamiyoga, Setagaya-ku, Tokyo 158-8501, Japan. Tel: 81-3-3700-9453. Fax: 81-3-5717-3832. E-mail: maekawa@nihs.go.jp

The channels are heteromeric assemblies composed of a pore forming α–subunit and a regulatory β–subunit. The gene encoding the α–subunit of the human cardiac Na$^+$ channel, *SCN5A*, consisting of 28 exons spanning approximately 80-kb, is located on chromosome 3p21 (Gellens *et al.* 1992; Wang *et al.* 1996). The α subunit is composed of 4 homologous domains (DI to DIV). Each domain consists of 6 transmembrane segments (S1 to S6) connected by linker segments.

Some inherited variations in *SCN5A* have been shown to cause severe disorders in cardiac rhythm that

require pacemaker or defibrillator implantation (Bezzina *et al.* 2001). These sodium channelopathies include the long QT syndrome type III (LQT-3) (Wang *et al.* 1995), Brugada syndrome (BrS) (Chen *et al.* 1998), idiopathic ventricular fibrillation (IVF) (Akai *et al.* 2000), sudden infant death syndrome (SIDS) (Ackerman *et al.* 2001) and cardiac conduction defects (CCD) (Schott *et al.* 1999). Electrophysiological studies on mutant Na^+ channels using heterologous expression systems have shown that the distinct effects of the mutant channels on the gating functions, and/or the difference in their availability, may result in these various clinical outcomes (Balser, 2001; Tan *et al.* 2003). Moreover, these genetic variations seem to modify responses to antiarrhythmic drug therapies, and in some cases to sensitize patients to the proarrhythmic effects of Na^+ channel-blocking antiarrhythmic drugs (Schwartz *et al.* 1995; Fujiki *et al.* 1999; Makita *et al.* 2002). As for the common single-nucleotide polymorphisms (SNPs) in *SCN5A*, they have also been shown to cause phenotypic variability of these channelopathies. For example, a common SNP, p.His558Arg, was reported to restore Na^+ channel function by counteracting the gating or trafficking defects caused by other variations (p.Thr512Ile and p.Met1766Leu) (Viswanathan *et al.* 2003; Ye *et al.* 2003). In contrast another SNP, p.Ser1102Tyr, which is frequently found in Africans, was reported to be a risk factor for arrhythmia (Splawski *et al.* 2002). Thus genetic variations, including common polymorphisms of *SCN5A*, affect cardiac electrophysiological properties in a wide range of arrhythmias, from the inherited sodium channelopathies to the common acquired rhythm disorders associated with coronary occlusion and structural heart disease.

In this study to elucidate the role of *SCN5A* variations in common cardiac rhythm disturbances in the Japanese population, all *SCN5A* coding exons and their flanking introns were sequenced in 166 Japanese arrhythmic patients who were not diagnosed with LQT or BrS, and in 232 healthy controls. We identified 69 genetic variations in *SCN5A*, including 12 novel missense variations, and then compared the frequencies of the SNPs and the haplotypes between the arrhythmic patients and the healthy controls.

Materials and Methods

Populations Studied and their Features

Unrelated Japanese arrhythmic patients (166) employed in this study were administered antiarrhythmic drugs (mexiletine, amiodarone, flecainide, or pilsicainide) at the National Cardiovascular Center (Suita, Japan). Informed consent was obtained from all patients. Genomic DNA was extracted from patient blood samples by standard protocols. Among the 166 patients, 126 were male with a mean age of 58 ± 11 years, and 40 were female with a mean age of 58 ± 13 years. Ventricular tachycardia was detected in 96 patients, premature ventricular contraction in 47 patients, atrial fibrillation and flutter in 36 patients, ventricular fibrillation in 16 patients, supraventricular tachycardia in 6 patients, and supraventricular premature contraction in 4 patients. As for the original causes of the arrhythmias, cardiomyopathy was observed in 78 patients, congestive heart failure in 28, myocardial infarction in 24, cornary artery disease (angina) in 18, valvular heart disease in 15, sarcoidosis in 7, and sick sinus syndrome in 4 patients. Arrhythmias were triggered by an unknown cause for 42 patients. Patients with LQT or BrS were not included in this study. Mexiletine, amiodarone, flecainide, and pilsicainide, were administered to 78 patients (100-450 mg/day), 89 patients (50–400 mg/day), 11 patients (100–200 mg/day), and 11 patients (50–150 mg/day), respectively. Twenty-two patients were administered both mexiletine and amiodarone. One patient was administered both flecainide and pilsicainide.

For the controls healthy subjects, with no history of syncope, ventricular tachycardia or ventricular fibrillation based on the medical examination, were recruited. Blood samples were collected from 232 healthy Japanese volunteers at the Tokyo Women's Medical University under the auspices of the Pharma SNP Consortium (Tokyo, Japan). Genomic DNA was extracted from Epstein-Barr virus-transformed lymphoblastoid cells. Informed consent was also obtained from all healthy subjects. Out of 232 healthy subjects, 135 were male with a mean age of 41±12 years, and 97 were female with a mean age of 37±13 years. The ethics committees of the National Cardiovascular Center, the

National Institute of Health Sciences, the Pharma SNP Consortium, and the Tokyo Women's Medical University approved this study.

Genetic Analysis of SCN5A

Genomic and cDNA sequences of *SCN5A* were obtained from GenBank (GenBank accession numbers NT·022517.16 and NM_198056.1, respectively). The genomic organization of *SCN5A* was deduced by comparing the cDNA with the genomic sequence. A glutamine residue at codon 1077 was numbered as the first amino acid residue of exon 18 according to NM_198056.1. This numbering was different from another reference sequence, NM_000335.3, a shorter 2015 amino acid splice variant which uses another potential acceptor site located 3-bp downstream from the original acceptor site of exon 18 and lacks the glutamine at position 1077 (1077delGln). According to Makielski *et al.* (2003), both splice variants with 2015 (65% of all transcripts) and 2016 amino acids residues (35% of all transcripts) are constitutively expressed.

PCR primers were designed in intronic regions to amplify all 27 coding exons (exons 2–28) (Table 1). The promoter regions and exon 1 were excluded because their structures were not fully characterized when this study began. Each exon was amplified by Ex-Taq (0.625 units) (Takara Shuzo, Tokyo, Japan) using the appropriate set of primers (0.2 μM) and genomic DNA (100 ng). The PCR conditions were 94°C for 5 min, followed by 30 cycles of 94°C for 30 sec, 61°C for 1 min, 72°C for 1.5 min, and a final extension at 72°C for 7 min. The PCR products were purified using a PCR Product Pre-Sequencing Kit (USB Co., Cleveland, OH) and were directly sequenced on both strands using an ABI BigDye Terminator Cycle Sequencing Kit (Applied Biosystems, Foster City, CA). The primers used to amplify each exon were also used for sequencing, except for the exons shown in Table 1. After the excess dye was removed with a DyeEx96 kit (Qiagen, Hilden, Germany), the eluates were analyzed on an ABI Prism 3700 DNA Analyzer (Applied Biosystems). The novel variations were confirmed by repeating the PCR on the genomic DNA and sequencing the subsequent PCR products.

Statistical Analysis

SNP frequencies in both of the groups were assessed for deviation from Hardy-Weinberg equilibrium using the χ^2 test. The observed allele frequencies were all in Hardy-Weinberg equilibrium except for c.4299+116G>A (data not shown). The reason for the significant deviation from Hardy-Weinberg equilibrium of c.4299+116G>A ($p = 0.002$ for total subjects, $p = 0.014$ for patients, and $p = 0.059$ for controls) is currently unknown. This SNP was omitted from the haplotype inference. The comparison of allele frequencies between the patients and healthy controls was performed using the χ^2 test or Fisher's exact test as appropriate, and the differences were considered to be significant when $p < 0.05$. Pairwise linkage disequilibrium (LD) between each SNP was calculated by r^2 statistics. These analyses were performed by the SNPAlyze software (DYNACOM CO., Ltd., Kanagawa, Japan). Haplotype frequencies and diplotype configurations were estimated by LDSUPPORT software (Kitamura *et al.* 2002) using an expectation-maximization (EM) algorithm. To examine the differences in the overall haplotype frequency profile between the patients and controls, the global permutation test was performed according to the methods of Zhao *et al.* (2000) using the software PM+EH+ version 1.2 (model free analysis and permutation tests for allelic associations, http://linkage.rockefeller.edu/soft/list.html). When the global permutation test showed significance between the two groups, the differences in individual haplotype frequencies were evaluated by χ^2 test or Fisher's exact test. In these tests, the frequency of one haplotype was compared with the combined frequencies of all the other haplotypes for the patients and controls.

Results

SCN5A Variations Found in a Japanese Population

All the *SCN5A* coding exons (exons 2-28) and their flanking introns were sequenced in 166 Japanese

Table 1 Primers used for amplification and sequencing of *SCN5A*

Exon	Forward primer (5' to 3')	Position[a]	Reverse primer (5' to 3')	Position[a]
2	GCAAATGGTGTCCCTCCCTC	38600581	ATGAGCCACCCTAAATAGAGC	38600037
	GGTCTGCCCACCCTGCTCTCT[b]	38600538		
3	GGGCAAGGCAGTGAGTCTAC	38597728	CTGGAGGAGGGTCAGAGGTT	38597234
			CTTAGGACCAGCAGGGAATC[b]	38597296
4	CAGCCCCAGTGTGTCTCCTT	38589746	GGCAGGACAGGGAGAAACTT	38589256
5	GAGCAAAGTTCCATCCCCAA	38588256	TGTCTCTCCCCACCAGGATG	38587773
6	ACTAGGCAATTTGTCGGCTC	38581161	ATGTCCACTGCCAATAGCCCC	38580702
	AGGTAAGATGCCCAGGTTTGCC[b]	38581092		
7	CCACCTCTGGTTGCCTACACTG	38577198	CTGTCCTCTGTCTGGGTCTCTG	38576709
	CACCCCAGCTCAACTCAGGC[b]	38577172	GGGATCAGGCAGGGCTTGAA[b]	38576732
8	GGCACTGGCAGCAGGATGTCT	38575550	GGGGTCAGGGCATAAATAGAA	38575170
	GGATGTCTTCAGAGGAACAG[b]	38575537		
9	CAGCGTGGCACTAGGTTTGT	38574074	AGTTTCTTTGCTGCTGATCC	38573618
10	TGGGACATCTCTACCCTCCT	38573396	CACCTATAGGCACCTACAGTCAG	38573004
11	GCCACTCCTATCTTCCTTCCTG	38572237	AACACCCAAAACTACCCTGT	38571668
	AAGTCACTGAGAGTTGCCTG[b]	38572112	GCTCCCCTACTCTAAGGAAG[b]	38571701
12	GCCCTCAATGCTCTGAGAAG	38571307	ACACAGTAGGTGCTCAACAA	38570719
13	CAGCATCCAGTGTCCCATCAAG	38566314	CAGTGTGGGGATGTCTAAAG	38565914
14	TCTCCCAGAGCAAGTCATAA	38565179	TGATTCCCACCCTCAAAAGA	38564714
15	CCACAGCCAAGCAAACCCCTA	38554839	GCCTTTCCTGCCTCTGTACC	38554327
16	GGGGGGAATAGGTGTCAGTG	38553289	GGGGGTAGGTGAAATAAATGAG	38552635
	TAGGTGTCAGTGCCCTCCAA[b]	38553281	CCAACTTACCACAAGGTTGC[b]	38552798
17	CCCTGGATTCAAGCCTCGGA	38548626	CTGTATATGTAGGTGCCTTATACATG	38548004
	CCTCAGTTTCCCCATCATAGAA[b]	38548571		
18	GGAGGAGTCTTCAGTGAGAT	38546762	TGACAGTGGCTGTGGCTCCCAA	38546340
			TGTGGCTCCCAACAGCAAAT[b]	38546350
19	TGACAGGCAAAAGTGGCTCT	38544061	ATCTAAGGCAGGGTGTTGGT	38543665
20	CTGCTCACCATATTGCCCTGTTC	38542709	GGGGGTCTGGAGAGCACATT	38542275
	GCCACCCCCATCATCGTAGCTC[b]	38542686		
21	GTGGCGGCAGGCATCTATAA	38533938	GCCTGGGTCACTCAGACTTACG	38533357
	AAATGGAAAGAAACGGTGCCTG[b]	38533782	ACTCAGACTTACGTCCTCCTTC[b]	38533366
22	CCCAGAAGCCAGGATACTCTTG	38529886	CCATGCTCCTACCAAGTCAGCC	38529388
23	CAGGGAGTTCATTCTTTCTTG	38527641	CCCTCTTCCTGCCCACATCAT	38527178
			CTGCCCACATCATGGGTGAT[b]	38527186
24	GTGAGGTGGGGTGGCTTGCTTT	38524528	AGGCTTGGGCATTCCAGAGA	38524191
25	ACACCCTCTTTCCCACAGAATG	38523817	GCAGGAGCAAGAAGAGGACCA	38523428
	ACAGAATGGACACCCCTAGAC[b]	38523803	CCAACAGGGAAGGTGAGATG[b]	38523452
26	GTGGTCAATCCTGGCATCCTCA	38522978	TTCCTCCCTATCTCTACGAG	38522595
27	TTTGGGCTCACTAGAGGGTAGA	38521785	CCCATTCCCAGACTCATCCTTG	38521076
28-1[c]	GCTCCTTGCCATATAGAGACC	38518782	GTGCTCTCCTCCGTGGCCACGC	38518140
	TGCACAGTGATGCTGGCTGGAA[b]	38518741	CAGTGTTGAGGATGGGGCTGAG[b]	38518318
28-2[c]	AAGTGGGAGGCTGGCATCGAC	38518441	CCGCCTGCTGACGGAAGAGGA	38517691
	TGGGAGGCTGGCATCGACGAC[b]	38518438		
28-3[c]	CCAACCAGATAAGCCTCATCAACA	38517999	AGCCCATTCACAACATATACAGTCT	38517122
	CATCCAAGATCTCCTACGAGCC[b]	38517837	CAGGCTGGTTTGTGACTGACTG[b]	38517351

[a]The nucleotide position of the 5' end of each primer on NT_022517.16.
[b]The primers used for sequencing were indicated only when they were different from those used to amplify each exon.
[c]Three sets of overlapping primers were used to amplify exon 28.

arrhythmic patients and 232 healthy controls. We found 69 genetic variations, including 54 novel ones. The positions and frequencies of all variations found in both the patients and healthy controls are shown in Table 2.

Of the 69 variations found in this study, 66 were single nucleotide polymorphisms (SNPs) and the remaining three were a deletion in intron 6 (c.611+76delC), an adenine base duplication in the polyadenine (poly A)

Table 2 Summary of variations in the *SCN5A* gene detected in Japanese arrhythmic patients and healthy controls

Location	Position[a]	Nucleotide alterations	Amino acid alterations[b]	Allele Frequency (patient)	Allele Frequency (healthy control)	Statistics cases/control[c]	References[d]
Intron 1	−64	T>C		0/332 (0)	1/464 (0.002)	–	*
Exon 2	c.30	C>T	p.Thr10Thr	0/332 (0)	1/464 (0.002)	–	*
	c.87	G>A	p.Ala29Ala	126/332 (0.380)	160/464 (0.345)	N.S.	NCBI
Intron 3	c.393−113	T>C		0/332 (0)	1/464 (0.002)	–	*
Exon 4	c.453	C>T	p.His151His	1/332 (0.003)	1/464 (0.002)	–	*
Intron 4	c.482+165	C>T		1/332 (0.003)	0/464 (0)	–	*
	c.482+184	A>G		164/332 (0.494)	211/464 (0.455)	N.S.	NCBI
	c.483−33	C>T		0/332 (0)	1/464 (0.002)	–	*
Exon 5	c.552	C>T	p.His184His	1/332 (0.003)	0/464 (0)	–	*
Intron 5	c.611+74	C>G		0/332 (0)	1/464 (0.002)	–	*
	c.611+76	delC		0/332 (0)	1/464 (0.002)	–	*
Intron 6	c.703+130	G>A		46/332 (0.139)	40/464 (0.086)	$p = 0.019$	*
Exon 7	c.714	C>T	p.Thr238Thr	1/332 (0.003)	0/464 (0)	–	*
	c.801	C>T	p.Ile267Ile	1/332 (0.003)	0/464 (0)	–	*
Intron 7	c.934+5	G>A		0/332 (0)	1/464 (0.002)	–	*
Intron 8	c.998+33	T>C		0/332 (0)	1/464 (0.002)	–	*
	c.999−28	G>A		0/332 (0)	1/464 (0.002)	–	*
Intron 9	c.1140+98	A>G		12/332 (0.036)	19/464 (0.041)	N.S.	NCBI
	c.1141−3	C>A		22/332 (0.066)	45/464 (0.097)	N.S	1
Exon 10	c.1282	G>A	**p.Glu428Lys**	0/332 (0)	1/464 (0.002)	–	*
Intron 10	c.1339−24	G>A		23/332 (0.069)	48/464(0.103)	N.S.	NCBI
Intron 11	c.1518+39	C>T		1/332 (0.003)	0/464 (0)	–	*
	c.1519−68	C>T		8/332 (0.024)	12/464 (0.026)	N.S.	*
Exon 12	c.1595	T>G	**p.Phe532Cys**	1/332 (0.003)	0/464 (0)	–	*
	c.1673	A>G	**p.His558Arg**	24/332 (0.072)	48/464 (0.103)	N.S.	NCBI
	c.1755	C>T	p.His585His	1/332 (0.003)	0/464 (0)	–	*
Intron 13	c.2023+32	C>T		1/332 (0.003)	0/464 (0)	–	*
Exon 14	c.2066	G>A	**p.Arg689His**	1/332 (0.003)	0/464 (0)	–	*
	c.2102	C>T	**p.Pro701Leu**	1/332 (0.003)	0/464 (0)	–	*
	c.2151	G>A	p.Pro717Pro	1/332 (0.003)	0/464 (0)	–	*
Intron 15	c.2263+39	G>A		1/332 (0.003)	0/464 (0)	–	*
Intron 17	c.3229-61	C>T		0/332 (0)	1/464 (0.002)	–	*
Exon 18	c.3269	C>T	**p.Pro1090Leu**	12/332 (0.036)	11/464 (0.024)	N.S.	NCBI
Intron 18	c.3391−70	C>T		1/332 (0.003)	0/464 (0)	–	*
Exon 19	c.3442	G>A	**p.Ala1148Thr**	0/332 (0)	1/464 (0.002)	–	*
Exon 20	c.3556	G>A	**p.Ala1186Thr**	0/332 (0)	1/464 (0.002)	–	*
	c.3578	G>A	**p.Arg1193Gln**	21/332 (0.063)	29/464 (0.063)	N.S.	2
	c.3598	C>T	**p.His1200Tyr**	1/332 (0.003)	0/464 (0)	–	*
Intron 20	c.3667−89	dupA		24/332 (0.072)	29/464 (0.063)	N.S.	*
Intron 21	c.3840+17	G>A		1/332 (0.003)	1/464 (0.002)	–	*
	c.3840+73	G>A		24/332 (0.072)	29/464 (0.063)	N.S.	*
	c.3840+76	C>T		1/332 (0.003)	0/464 (0)	–	*
Intron 23	c.4246-7	C>A		0/332 (0)	1/464 (0.002)	–	*
Intron 24	c.4299+53	T>C		88/332 (0.265)	128/464 (0.276)	N.S.	3
	c.4299+116	G>A		36/332 (0.108)	47/464 (0.101)	N.S	*
Exon 25	c.4302	T>C	p.Tyr1434Tyr	0/332 (0)	3/464 (0.006)	–	*
Intron 25	c.4437+45	C>T		0/332 (0)	1/464 (0.002)	–	*
Intron 26	c.4542+86	A>G		38/332 (0.114)	52/464 (0.112)	N.S	*
	c.4543−30	T>G		0/332 (0)	1/464 (0.002)	–	*
Intron 27	c.4813 + 24	G>A		3/332 (0.009)	2/464 (0.004)	–	*
	c.4813+164	C>G		38/332 (0.114)	52/464 (0.112)	N.S.	NCBI
	c.4813+215	T>C		38/332 (0.114)	52/464 (0.112)	N.S.	NCBI
	c.4813+262	A>C		38/332 (0.114)	52/464 (0.112)	N.S.	NCBI

Table 2 Continued

Location	Position[a]	Nucleotide alterations	Amino acid alterations[b]	Allele Frequency (patient)	Allele Frequency (healthy control)	Statistics cases/control[c]	References[d]
	c.4814−80	C>A		0/332 (0)	6/464 (0.013)	–	*
Exon 28	c.4851	C>T	p.Phe1617Phe	0/332 (0)	1/464 (0.002)	–	*
	c.4999	G>A	**p.Val1667Ile**	1/332 (0.003)	0/464 (0)	–	*
	c.5082	C>T	p.Phe1694Phe	0/332 (0)	1/464 (0.002)	–	*
	c.5216	G>A	**p.Arg1739Gln**	1/332 (0.003)	0/464 (0)	–	*
	c.5457	T>C	p.Asp1819Asp	164/332 (0.494)	230/464 (0.496)	N.S.	NCBI
	c.5737	C>T	**p.Arg1913Cys**	0/332 (0)	1/464 (0.002)	–	*
	c.5775	C>G	p.Ser1925Ser	1/332 (0.003)	2/464 (0.004)	–	*
	c.5795	C>T	**p.Ala1932Val**	0/332 (0)	1/464 (0.002)	–	*
	c.5851	G>T	**p.Val1951Leu**	1/332 (0.003)	2/464 (0.004)	–	3,4
	c.5963	T>G	**p.Leu1988Arg**	1/332 (0.003)	11/464 (0.024)	$p = 0.018$	*
3'-UTR	c.6056	C>T		0/332 (0)	1/464 (0.002)	–	*
	c.6122−6125	dupGTCA		2/332 (0.006)	1/464 (0.002)	–	*
	c.6155	G>C		1/332 (0.003)	0/464 (0)	–	*
	c.6174	A>G		163/332 (0.491)	229/464 (0.494)	N.S	NCBI
	c.6255	T>C		1/332 (0.003)	9/464 (0.019)	N.S.	*

[a]cDNA numbers are relative to the ATG start site and based on the cDNA sequence (NM_198056.1).
[b]Non-synonymous changes are shown in **bold**.
[c]p value of χ^2 test or Fisher's exact test for allele was shown. N.S.: not significant ($p \geqq 0.05$).
[d]* indicates a novel variation. "NCBI" denotes the SNPs that have already published in the dbSNP database of the National Center for Biotechnology Information. NCBI SNP cluster ID (rs#) of these SNPs are as follows; c.87G>A, p.Ala29Ala (rs6599230); c.482+184A>G (rs6781731); c.1140+98A>G (rs6599222); c.1339−24G>A (rs7428779); c.1673A>G, p.His558Arg (rs1805124); c.3269C>T, p.Pro1090Leu (rs1805125); c.4813+164C>G (rs7429347); c.4813+215T>C (rs7431641); c.4813+262A>C (rs7432127); c.5457T>C, p.Asp1819Asp (rs1805126); c.6174A>G (rs7429945).
The other SNPs that were reported elsewhere are as follows:
1, Schulze-Bahr *et al.* [2003], 2, Vatta *et al.* [2002], 3, Iwasa *et al.* [2000], 4, Priori *et al.* [2002].

tract of intron 20 (c.3667-89dupA), and a 4-nucleotide duplication in the 3'-untranslated region (3'-UTR, c.6122− 6125dupGTCA). Of the 66 SNPs, 29 were located in the coding exons (13 synonymous and 16 non-synonymous), 33 in the introns, and 4 in the 3'-UTR.

The 54 novel variations included twelve nonsynonymous SNPs. One SNP, c.5963T>G (p.Leu1988 Arg), was heterozygous in eleven healthy subjects and only one patient. Five SNPs, c.1282G>A (p.Glu428Lys), c.3442G>A (p.Ala1148Thr), c.3556 G>A (p.Ala1186Thr), c.5737C>T (p.Arg1913Cys), and c.5795C>T (p.Ala1932Val), were heterozygous in 5 different healthy controls. The remaining six non-synonymous SNPs, c.1595T>G (p.Phe532Cys), c.2066 G>A (p.Arg689His), c.2102C>T (p.Pro701Leu), c.3598C>T (p.His1200Tyr), c.4999G>A (p.Val 1667Ile), and c.5216G>A (p.Arg1739Gln), were found separately in six arrhythmic patients, but not in healthy controls. The locations corresponding to

the 16 nonsynonymous SNPs in the SCN5A protein are depicted in Figure 1. Table 3 summarizes the clinical characteristics of the individuals with the novel nonsynonymous SNPs.

Fifteen previously reported variations were detected in our study. They included four coding SNPs (cSNP), c.87G>A (p.Ala29Ala), c.1673A>G (p.His558Arg), c.3269C>T (p.Pro1090Leu), and c.5457T>C (p.Asp1819Asp), and seven non-coding SNPs (c.482+184A>G, c.1140+98A>G, c.1339– 24G>A, c.4813+164C>G, c.4813+215T>C, c.4813+ 262A>C, and c.6174A>G), which were published in the dbSNP database of the National Center for Biotechnology Information (NCBI) (http://www.ncbi. nlm.nih.gov/SNP/index.html). Two SNPs, c.4299+53T>C and c.5851G>T (p.Val1951Leu), were previously identified in Japanese individuals by Iwasa *et al.* (2000). The remaining 2 SNPs were c.1141-3C>A (Schulze-Bahr *et al.* 2003) and
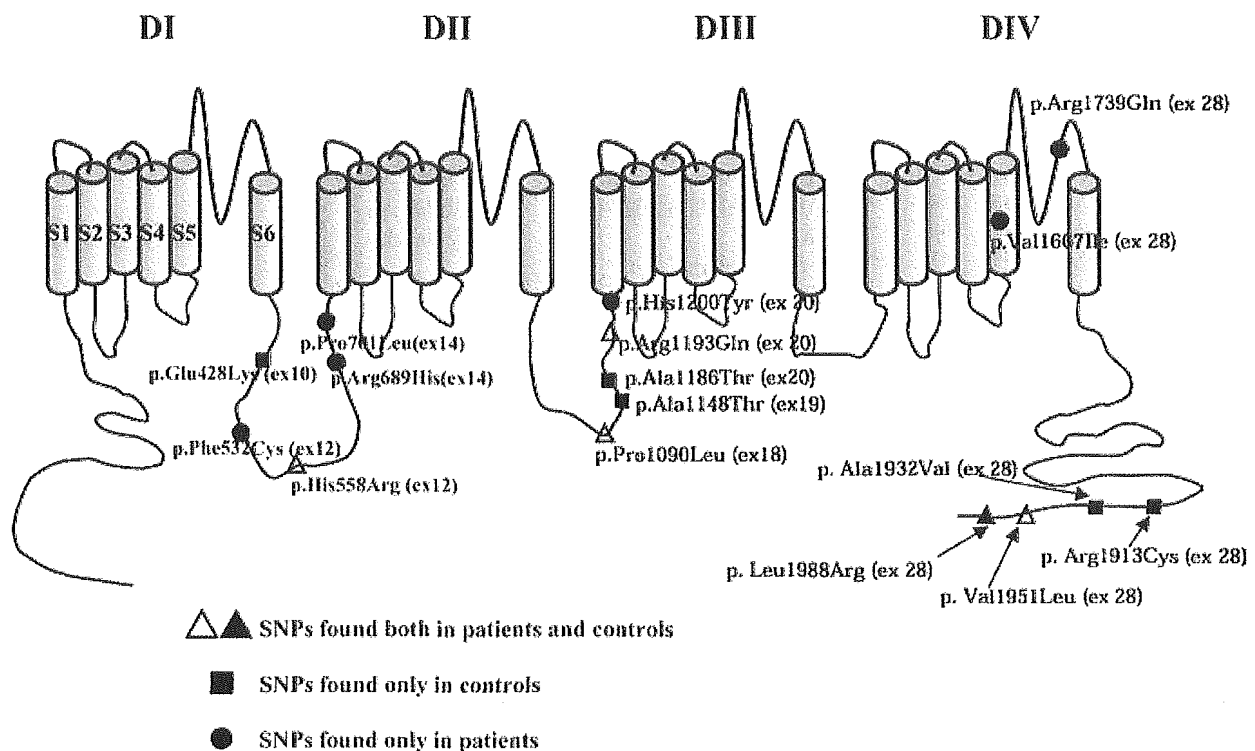
Figure 1 Sixteen nonsynonymous SNPs identified in the Japanese population in this study are depicted on the predicted topology of the *SCN5A* protein. One novel and four known nonsynonymous SNPs, found both in controls and patients, are indicated by an open triangle and closed triangle, respectively. Five novel nonsynonymous SNPs found only in controls are indicated by a closed square. Six novel nonsynonymous SNPs found only in patients are shown by a closed circle.

c.3578G>A (p.Arg1193Gln) (Vatta *et al.* 2002). The allele frequencies of c.5457C>T (p.Asp1819Asp) (0.50) and c.4299+53T>C (0.27) were similar to those (0.46 and 0.27, respectively) found in a Japanese population and reported by Iwasa *et al.* (2000). The frequencies of c.87G>A (p.Ala29Ala) (0.35) and c.1141-3C>A (0.10) for healthy controls were comparable to those (0.28 and 0.16, respectively) for 32 healthy Caucasians as reported by Paulussen *et al.* (2004).

On the other hand, we failed to detect the seven SNPs reported in the dbSNP database; c.100C>T (p.Arg34Cys; rs6791924), c.274–25G>A (rs7636280), c.274–24C>T (rs7627488), c.1654G>C (p.Gly552Arg; rs3918389), c.2437–97C>T (rs7645173), c.3183A>G (p.Glu1061Glu; rs7430407), and c.3305C>A (p.Ser1102Tyr; rs7626962). Splawski *et al.* (2002) reported that p.Ser1102Tyr is a common variation of *SCN5A* in

Africans at allele frequencies of 0.13–0.19, but is not found in Caucasians and Asians. p.Arg34Cys was found in a U.S. population at an allele frequency of 0.04 (Yang *et al.* 2002). Lastly, Paulussen *et al.* (2004) reported that the allele frequencies of c.274–24C>T and p.Glu1061Glu were 0.02 and 0.13, respectively, in 32 healthy Caucasians. Thus, they seem to be either ethnic-specific or rare.

Of the 69 variations, 22 were polymorphisms and detected with minor allele frequencies over 1% (more than 8 chromosomes from a total of 398 subjects). To determine whether these relatively frequent polymorphisms were associated with cardiac arrhythmias, their allele frequencies were compared between the patients and controls. Two out of the 22 SNPs showed significantly different frequencies between the patient and control groups ($p < 0.05$). The patients were more likely to have the c.703+130A allele compared with the healthy controls, with an odds ratio of 1.70 (95%

Table 3 Clinical characteristics of the arrhythmic patients and healthy individuals bearing novel nonsynonymous SNPs

Novel nonsynonymous SNPs	Age (years)	Sex	Diagnosis[a]	Medication[b]	Other nonsynonymous SNPs detected in the same subject[c]
c.1282G>A (p.Glu428Lys)	21	F	control subject	No	ND
c.1595T>G (p.Phe532Cys)	58	M	Paf, AT, MS	AMD 200 mg/day	ND
c.2066G>A (p.Arg689His)	54	M	VT, mitral valvular disease	MEX 300mg/day	ND
c.2102C>T (p.Pro701Leu)	60	M	Af	PIL 150 mg/day	c.5851G>T; p.Val1951Leu (hetero)
c.3442G>A (p.Ala1148Thr)	47	M	control subject	No	ND
c.3556G>A (p.Ala1186Thr)	42	M	control subject	No	ND
c.3598C>T (p.His1200Tyr)	36	M	VF, HCM	AMD 100 ng/day	ND
c.4999G>A (p.Val1667Ile)	66	F	VT	AMD 200mg/day	c.3269C>T; p.Pro1090Leu (hetero)
c.5216G>A (p.Arg1739Gln)	35	M	DCM, CHF	AMD 100 mg/day	c.1673A>G; p.His558Arg (hetero)
c.5737C>T (p.Arg1913Cys)	48	M	control subject	No	c.3578G>A; p.Arg1193Gln (hetero)
c.5795C>T (p.Ala1932Val)	35	M	control subject	No	ND
c.5963T>G (p.Leu1988Arg)	47	M	DCM, nonsustained VT, CHF, myocardial sarcoidosis	AMD 150 mg/day	c.1673A>G; p.His558Arg (homo)
	37	F	control subject	No	c.1673A>G; p.His558Arg (hetero)
	58	M	control subject	No	c.1673A>G; p.His558Arg (hetero)
	34	M	control subject	No	c.1673A>G; p.His558Arg (hetero)
	41	M	control subject	No	c.1673A>G; p.His558Arg (hetero)
	45	M	control subject	No	c.1673A>G; p.His558Arg (hetero)
	47	M	control subject	No	c.1673A>G; p.His558Arg (hetero)
	31	F	control subject	No	c.1673A>G; p.His558Arg (homo)
	35	F	control subject	No	c.1673A>G; p.His558Arg (hetero)
	30	F	control subject	No	c.1673A>G; p.His558Arg (hetero)
	21	M	control subject	No	c.1673A>G; p.His558Arg (hetero)
	28	M	control subject	No	c.1673A>G; p.His558Arg (hetero), 3578G>A; Arg1193Gln (hetero)

[a]Paf, paroxysmal atrial fibrillation; AT, atrial tachycardia; MS, mitral stenosis; VT, ventricular tachycardia; Af, atrial fibrillation; VF, ventricular fibrillation; HCM, hypertrophic cardiomyopathy; DCM, dilated cardiomyopathy; CHF, congestive heart failure
[b]MEX, mexiletine; AMD, amiodarone; PIL, pilsicainide
[c]ND; not detected

confidence interval [95% CI] 1.07–2.65) and χ^2 of 5.50 ($p = 0.019$). In contrast, the allele frequency of c.5963T>G (p.Leu1988Arg) was significantly lower in the patients than in the controls (odds ratio = 0.124 [95% CI] 0.00–0.53, $p = 0.018$ by Fisher's exact test). As for the other 20 variations, no significant differences were found between the allele frequencies of the patients and healthy controls.

In our study, the control subjects (mean age, 40 ± 12 years) were relatively young compared with the arrhythmic patients (mean age, 58 ± 12 years). To evaluate the influence of age differences on our association results, we divided both the patients and healthy controls into three subgroups by age (i.e., 20–39, 40–59 and 60–80 years). Both c.703+130G>A and p.Leu1988Arg were detected at almost equal frequencies among the three age subgroups within each group (data not shown),

indicating that the allele frequencies in either group were not influenced by the age of the subjects.

Linkage Disequilibrium (LD) Analysis

Pairwise LD was calculated between the 22 polymorphisms (minor allele frequency > 1.0%). The pairs that have r^2 values over 0.1 are shown in Figure 2. Strong LDs were found in four SNP groups: c.1141−3C>A, c.1339-24G>A, and c.1673A>G (p.His558Arg) (r^2 > 0.92); c.4542+86A>G, c.4813+164C>G, c.4813+215T>C, and c.4813+262A>C ($r^2 = 1.0$); c.5457T>C (p.Asp1819Asp) and c.6174A>G ($r^2 = 0.99$); c.5963T>G (p.Leu1988Arg) and c.6255T>C ($r^2 = 0.83$). Moderate LD was observed between c.4299+53T>C and c.5457T>C (p.Asp1819Asp) ($r^2 = 0.37$), between c.4299+53T>C and c.6174A>G ($r^2 = 0.37$), between c.3269C>T (p.Pro1090Leu) and c.3840+73G>A ($r^2 = 0.27$), and between c.1519−68C>T and c.3667−89dupA ($r^2 = 0.25$).
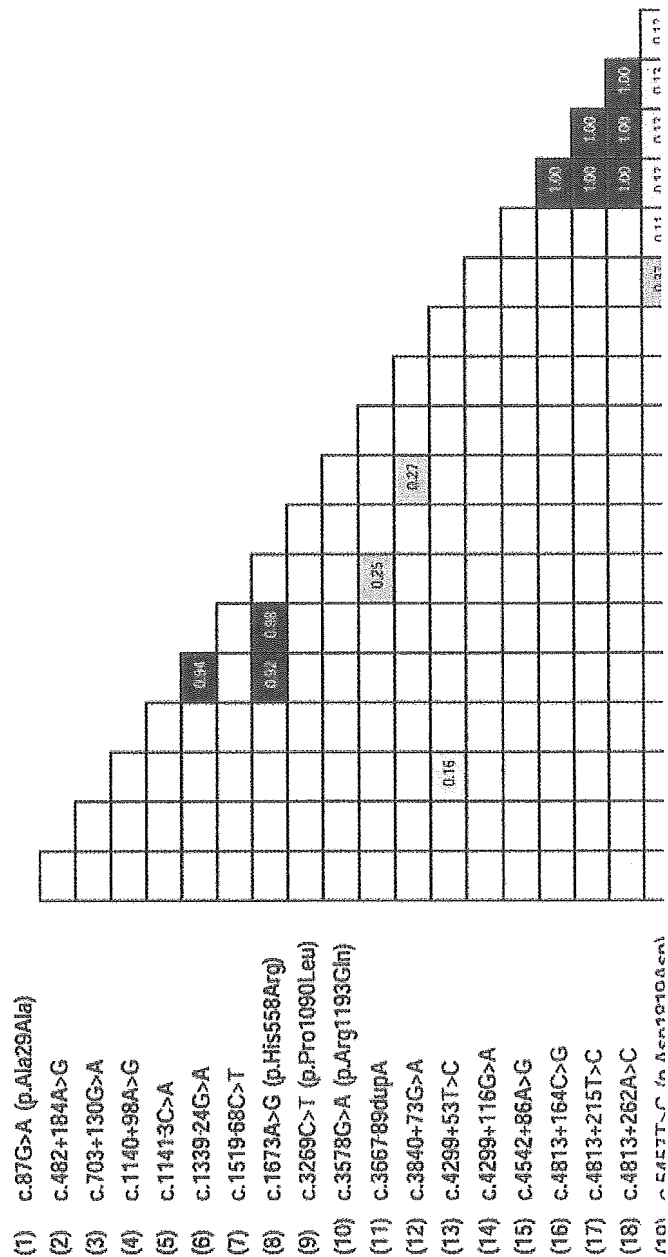
Figure 1 also illustrates the positions of the 22 variations. For subsequent analysis of *SCN5A* haplotype structures we assigned 5 LD blocks, so that the closely associated SNPs ($\rho^2 > 0.20$) could be grouped together. Blocks 1, 2 and 3 included only a single SNP, c.87G>A (p.Ala29Ala), c.482+184A>G, and c.703+130G>A, respectively, because these SNPs showed little LD ($\rho^2 < 0.20$) with the other variations. Block 4, spanning 40 kb (from introns 9 to 21), included 9 variations (c.1140+98A>G, c.1141–3C>A, c.1339–24G>A, c.1519–68C>T, c.1673A>G; p.His558Arg, c.3269C>T; p.Pro1090Leu, c.3578G>A; p.Arg1193Gln, c.3667–89dupA, c.3840+73G>A). The remaining 10 variations (c.4299+53T>C, c.4299+116G>A, c.4542+86A>G, c.4813+164C>G, c.4813+215T>C, c.4813+262A>C, c.5457T>C; p.Asp1819Asp, c.5963T>G; p.Leu1988Arg, c.6174A>G, c.6255T>C) were assigned to block 5, ranging from intron 24 to exon 28 (7 kb).

Haplotypes and their Associations with Arrhythmogenesis

First, the haplotype frequencies for the blocks were evaluated. For blocks 1 to 3, the haplotype frequencies were the same as the allele frequencies of the single SNPs. Therefore, significant differences in haplotype (allele) frequencies were found only in block 3 (c.703+130G>A) as described above. In block 4, eight common haplotypes were inferred with frequencies over 1% (* *1a*-* *1e*, * *2a*, * *3a* and * *4a*), accounting for 97% of all the observed haplotypes (Table 4a). In block 5, five common haplotypes with frequencies over 1% (* *1a*-* *1d*, and * *2a*) accounted for 99% of all the inferred haplotypes (Table 4b). The frequency of the block 5 * *2* haplotype (* *2a* and * *2b*) bearing c.5963T>G (p.Leu1988Arg) was about eight times higher in the controls than in the patients. For the other haplotypes in blocks 4 and 5, however, no significant differences in haplotype frequencies between the patients and controls were obtained.

Next, the combinations of in-block haplotypes (inter-block haplotypes; e.g., block1 * *1a* - block2 * *1a* – block3 * *1a* – block4 * *1a* – block5 * *1a*) were assessed. However, there were too many inter-block haplotypes, each having low frequencies, to obtain statistical significance by comparing them between the patients and controls. Nonetheless, the haplotypes harbouring the

SNPs c.703+130G>A or c.5963T>G (p.Leu1988Arg), which showed significant differences in allele frequencies between the patients and controls, showed unique linkages beyond the blocks. The * *2* haplotypes (* *2a* and * *2b*) in block 5 were always associated with the * *2a* haplotype in block 4, which harbours 3 linked SNPs, including the nonsynonymous SNP c.1673A>G (p.His558Arg). The SNP c.703+130G>A in block 3 was mostly associated with * *1b* in block 5, which harboured three SNPs including c.4299+53T>C. Thus, in spite of recombination between LD blocks, some block haplotype combinations were sustained. To assess the association between these inter-block haplotypes and risk of arrhythmias, we then applied the permutation and model-free analysis and estimation haplotype (PM+EM+) methods using the two haplotype-tagging SNPs c.1673A>G (p.His558Arg) and c.5963T>G (p.Leu1988Arg) or c.703+130G>A and c.4299+53T>C. (Table 5).

When the combinations between c.1673A>G (p.His558Arg) and c.5963T>G (p.Leu1988Arg) were analyzed, 3 haplotypic combinations were inferred in both of the two groups. The haplotype AG (558His-1988Arg) was completely absent in both groups, and the haplotype GG (558Arg-1988Arg) was present less frequently in the patients compared to the healthy controls. The global permutation test indicated that there was a significant difference in distribution of the haplotypes between the patients and controls ($\chi^2 = 7.42$, $p = 0.0260$). In accordance with this result, the frequency of haplotype GG (558Arg-1988Arg) was significantly lower in the patients than in the controls ($p = 0.018$).

As for the 4 haplotypes estimated from c.703+130G>A and c.4299+53T>C, haplotype AT was about 3 times as frequent in the patients as in the controls. However, the global difference between the patients and controls had a borderline significance ($\chi^2 = 8.64$, $p = 0.0550$) by the global permutation test.

Discussion

Since the defect in *SCN5A* was first reported to be a cause of LQT-3 (Wang *et al.* 1995), a variety of genetic alterations in *SCN5A* have been suggested to influence the pathophysiology of cardiac arrhythmias and/or pharmacological sensitivities to antiarrhythmic drugs. In this study we comprehensively searched for

Table 4 Haplotypes of blocks 4 and 5 and their frequencies in *SCN5A* for Japanese arrhythmic patients and healthy controls

a) block 4

Exon/Intron	Intron 9	Intron 9	Intron 10	Intron 11	Exon 12	Exon 18	Exon 20	Intron 20	Intron 21		Frequency (%)		
Position (NT_022517.16)	g.38573687	g.38573267	g.38572048	g.38571267	g.38571045	g.38546571	g.38542501	g.38533787	g.38533452		All subjects	Patients	Controls
Position (NM_198056.1)	c.1140 + 98	c.1141 − 3	c.1339 − 24	c.1519 − 68	c.1673	c.3269	3578	c.3667 − 89	c.3840 + 73				
Nucleotide change	A>G	C>A	G>A	C>T	A>G	C>T	G>A	dupA	G>A				
Amino acid change					His558Arg	Pro1090Leu	Arg1193Gln						
Haplotypes[a]													
*1 *1a											68.22	69.57	68.50
*1b											4.11	3.88	3.92
*1c											3.80	4.45	2.94
*1d											3.73	3.54	3.40
*1e											1.94	1.78	1.82
*1f											0.29	0.32	0.26
*2 *2a											7.41	5.36	8.58
*2b											0.47	0.26	0.71
*2c											0.40	0.30	0.45
*3 *3a											6.06	6.04	5.53
*4 *4a											2.09	2.59	1.56
*4b											0.29	0.32	0.25
*5 *5a											0.28	0.70	0.02
Others with frequencies less than 0.25 %											0.91	0.89	2.06

b) block 5

Exon/Intron	Intron 24	Intron 26	Intron 27	Intron 27	Intron 27	Exon 28	Exon 28	Exon 28 (3′-UTR)	Exon 28 (3′-UTR)		Frequency (%)		
Position (NT_022517.16)	g.38524294	g.38522686	g.38521231	g.38521180	g.38521133	g.38518031	g.38517525	g.38517314	g.38517233		All subjects	Patients	Controls
Position (NM_198056.1)	c.4299 + 53	c.4542 + 86	c.4813 + 164	c.4813 + 215	c.4813 + 262	5457	5963	c.6174	c.6255				
Nucleotide change	T>C	A>G	C>G	T>C	A>C	T>C	T>G	A>G	T>C				
Amino acid change						Asp1819Asp (silent)	Leu1988Arg						
Haplotypes[a]													
*1 *1a											48.85	50.30	47.82
*1b											26.99	26.51	27.35
*1c											11.31	11.45	11.21
*1d											10.95	11.14	10.80
*1e											0.25	0.30	0.22
*2 *2a											1.26	0.30	1.94
*2b											0.25	0.00	0.43
Others with frequencies less than 0.25 %)											0.14	0.00	0.23

[a]The wild-type haplotype was designated as * *1* , and the nonsynonymous SNP-bearing haplotypes were numerically defined. The subtypes were named with small alphabetical letters in the order of their frequencies.

White cells indicate major allele, and ▨ indicate minor allele.

The haplotypes found in two or more chromosomes (frequencies>0.25%) were shown.